Materials Science and Engineering B 163 (2009) 44–47

Contents lists available at ScienceDirect

Materials Science and Engineering B

journal homepage: www.elsevier.com/locate/mseb

# Annealing effects of $Ga_2O_3$–ZnO core-shell heteronanowires

Hyoun Woo Kim*, Jong Woo Lee, Mesfin Abayneh Kebede, Hyo Sung Kim, Chongmu Lee

*Division of Materials Science and Engineering, Inha University, 253 Yong Hyun Dong, Nam Gu, Incheon 402-751, Republic of Korea*

ARTICLE INFO

*Article history:*
Received 17 July 2008
Received in revised form 9 April 2009
Accepted 21 April 2009

*Keywords:*
A. Fibres
B. Thermal properties
D. Transmission electron microscopy (TEM)
D. X-ray diffraction (XRD)
E. Annealing

ABSTRACT

We prepared ZnO-coated $Ga_2O_3$ nanowires and investigated changes in the morphological, structural, and photoluminescence (PL) characteristics resulting from application of a thermal annealing process. With the thermal annealing at 800 °C, defect-associated PL peaks (2.2 and 2.6 eV) have been intensified with respect to the UV peak, and a new 2.8 eV-peak has been generated. Possible emission mechanisms are also discussed.



## 1. Introduction

Zinc oxide (ZnO) has been widely studied due to its useful optical functions based on the large binding energy of excitons and biexcitons (60 and 15 meV, respectively) as well as its multi-functional physical properties. In addition, ZnO nanowires have been utilized for fabricating field effect transistors [1], nanocantilevers [2], and nanoresonators [3]. Gallium oxide ($Ga_2O_3$), meanwhile, is an attractive material for application in gas sensors, transparent conductors, and phosphors. It is anticipated that $Ga_2O_3$ will be employed in new generation optoelectronic devices, including flat-panel displays, optical emitters, and solar cells, due to its extraordinary conduction and luminescence properties [4,5].

In recent years, coaxial nanocable-like one-dimensional (1D) structures have garnered considerable attention for a diverse range of applications [6–13]. For the present study on annealing effects, we coated ZnO on the surface of $Ga_2O_3$ nanowires via an atomic layer deposition (ALD) technique [14], producing nanoscaled layers with precisely controlled thickness and excellent conformability [15–17]. Herein, we comparatively scrutinized the core/shell structures before and after thermal annealing, in regard to their structural and photoluminescence (PL) properties. To the best of our knowledge, this is the first report on the annealing effects of $Ga_2O_3$/ZnO core-shell structures. Given the extraordinary physical and chemical properties of the oxides $Ga_2O_3$ and ZnO, it is anticipated that nanowire heterostructures consisting of these materials will find a variety of applications such as optoelectronics, sensors, etc.

## 2. Experimental

$Ga_2O_3$ core nanowires were synthesized in a metalorganic chemical vapor deposition system. Details of the experimental apparatus have been described elsewhere [18]. We employed Si(1 0 0) substrates, which were chemically cleaned with acetone ($CH_3COCH_3$) and water. In the growth process, where TMGa and oxygen ($O_2$), respectively, were used as gallium and oxygen sources, the substrate was set at 600 °C for 5 min [19].

Atomic layer deposition of ZnO shell layers on core $Ga_2O_3$ nanowires was carried out using diethylzinc (DEZn) and $H_2O$ as Zn and O precursors, respectively, in bubblers at 10 °C [20]. The pulse period was 0.2 s for the precursors and 2 s for the purge time between the reactants. With the ALD cycle number of 50, the substrate temperature was set at 150 °C. Following this, samples were annealed thermally at 800 °C in $N_2$ ambient for 0.5 h (flow rate: 500 standard $cm^3$/min).

The core/shell structures were characterized by X-ray diffraction (XRD) (Philips X'pert MRD diffractometer with Cu $K\alpha_1$ radiation), scanning electron microscopy (FE-SEM) (Hitachi, S-4200), and transmission electron microscopy (TEM) (Philips, CM-200), where the TEM was equipped with an energy dispersive X-ray spectroscope (EDX). PL was conducted at room temperature with the 325 nm line from a He–Cd laser (Kimon, 1K, Japan).

## 3. Results and discussion

Fig. 1a shows a SEM image of $Ga_2O_3$–ZnO core-shell structures that have been annealed at 800 °C, revealing 1D structures. Fig. 1b shows an enlarged SEM image, which shows that the nanowires exhibit a slightly rough surface. Since the core/shell nanowires exhibited a rough surface prior to thermal annealing (inset of

* Corresponding author.
*E-mail address:* hwkim@inha.ac.kr (H.W. Kim).

0921-5107/$ – see front matter © 2009 Elsevier B.V. All rights reserved.
doi:10.1016/j.mseb.2009.04.018

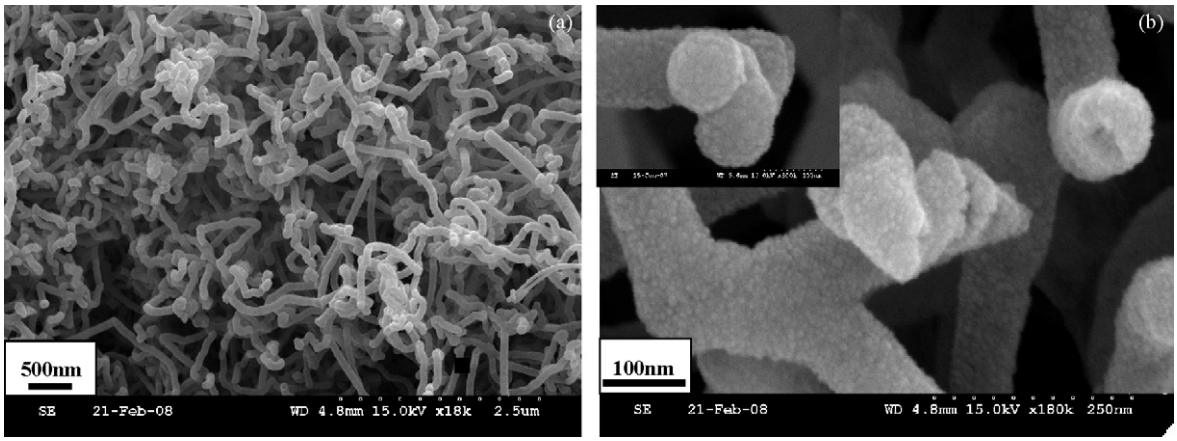


**Fig. 1.** (a, b) SEM images of core/shell structures annealed at 800 °C (inset: SEM image of the core/shell structures prior to thermal annealing).

Fig. 1b), we surmise that the surface roughness originated from the as-deposited shell layer.

Fig. 2a shows a low-magnification TEM image of a core/shell nanowire prior to thermal annealing. The upper left inset of Fig. 2a shows the selected area electron diffraction (SAED) pattern. Our previous experiments revealed that core $Ga_2O_3$ nanowires are amorphous [18]. Accordingly, weak diffraction rings correspond to the ZnO shell layer. The diffusive rings from inside to outside belong to (1 0 0), (1 0 1), (1 0 2), (1 0 3), and (1 1 2) planes of hexagonal ZnO, respectively. On the other hand, the observed halo presumably originated from the $Ga_2O_3$ core and ZnO shell layer. The lower right inset in Fig. 2a shows a lattice-resolved TEM image enlarging an

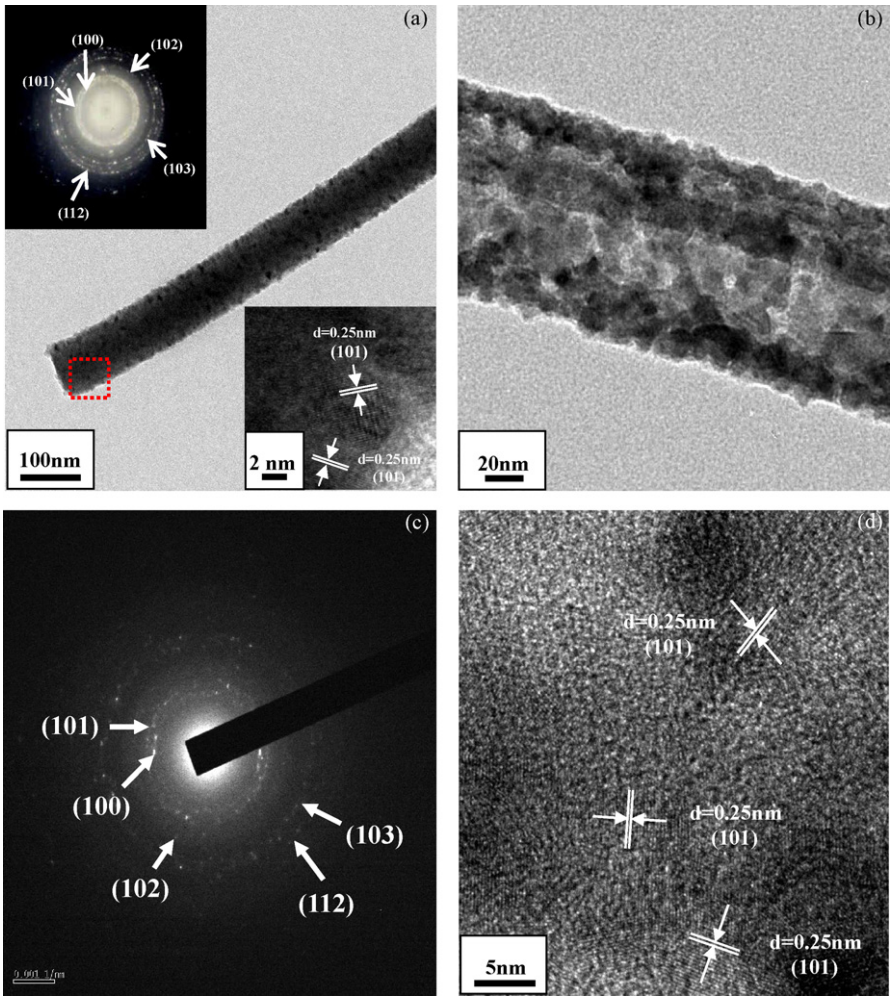


**Fig. 2.** (a) Low-magnification TEM image of a core/shell nanowire prior to thermal annealing. The upper left inset shows the SAED pattern. The lower right inset shows a lattice-resolved TEM image enlarging an area enclosed by the square box in (a) (from Ref. [14]). (b) Low-magnification TEM image of an annealed core/shell nanowire. (c) The SAED pattern shows that the annealed product is composed of amorphous and crystalline phases. (d) Lattice-resolved TEM image, exhibiting both crystalline and amorphous phases.

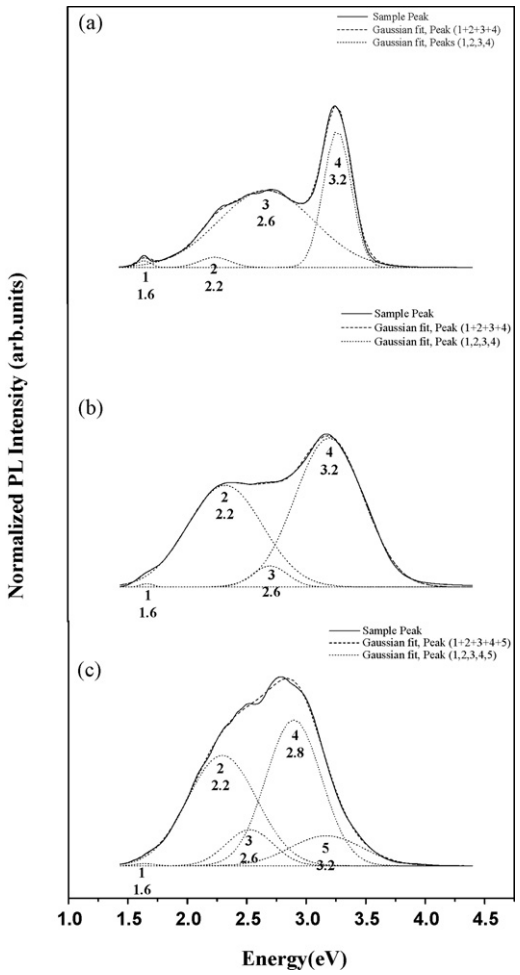


**Fig. 3.** Normalized PL spectra of (a) core $Ga_2O_3$ nanowires, (b) ZnO-coated $Ga_2O_3$ nanowires prior to thermal annealing, and (c) ZnO-coated $Ga_2O_3$ nanowires after thermal annealing.

area enclosed by the square box in Fig. 2a. The observed interplanar spacings are about 0.25 nm, and belong to the (1 0 1) plane of hexagonal ZnO. The lattice-resolved TEM image reveals that the shell layer of the coated nanowire comprises a crystalline phase.

Fig. 2b shows a low-magnification TEM image of an annealed core/shell nanowire, indicating that the shell layer has some degree of surface roughness. The SAED pattern shown in Fig. 2c reveals that the annealed product is composed of amorphous and crystalline phases. Existence of weak diffraction rings suggests that the ZnO shell layer contains a crystalline phase. Fig. 2d shows a typical lattice-resolved TEM image, exhibiting the crystalline ZnO phase.

The PL spectrum of the core $Ga_2O_3$ nanowires is presented in Fig. 3a. Through peak-deconvolution into Gaussian distribution functions, it is revealed that the PL spectrum consists of four emission bands, at 3.2, 2.6, 2.2, and 1.6 eV. The blue emission band at 2.6 eV is known to be associated with defects including oxygen vacancies and gallium vacancies [4,21]. The blue emission around 2.6 eV has previously been found from $Ga_2O_3$ nanowires [22,23]. The UV emission around 3.2 eV is attributed to the presence of self-trapped excitons, where recombination occurs [22,23]. The green emission band or peak has been observed from $Ga_2O_3$ nanobelts [24], $Ga_2O_3$ nanowires [22], and $Ga_2O_3$–ZnO coaxial nanocables [25]; however its mechanism has not been revealed. In addition, we observe a red band centered at around 1.6 eV. It is known that nitrogen impurities in $Ga_2O_3$ facilitate the generation of hole traps [26]. The holes recombine with electrons in oxygen vacancies, producing red emission. We surmise that intrinsic nitrogen impurities or nitrogen incorporation during the evaporation process under the $N_2$ gas flow can be a source of nitrogen in $Ga_2O_3$.

Fig. 3b shows a deconvoluted PL spectrum of the ZnO-coated $Ga_2O_3$ nanowires, exhibiting emission bands at 3.2, 2.6, 2.2, and 1.6 eV. Comparing Fig. 3b with Fig. 3a, it is found that the relative intensity of the 2.2 eV-peak and 3.2 eV-peak has been increased by the ZnO coating. While some peaks (2.6 and 1.6 eV) are mainly associated with core $Ga_2O_3$ nanowires, the green and UV emissions from core $Ga_2O_3$ nanowires have apparently been overlapped with those from ZnO shell layers. It is known that the green emission of ZnO results from deep trapping sites arising from possible defects such as oxygen vacancies [27–31]. Also, the UV emission of ZnO results from an emission mechanism associated with excitons in ZnO [29,30].

Fig. 3c shows the PL spectrum of ZnO-coated $Ga_2O_3$ nanowires that have undergone a subsequent thermal annealing procedure. Apart from emission bands peaked at 3.2, 2.6, 2.2, and 1.6 eV, there exists an emission band peaked at 2.8 eV. Since the origin of the 2.8 eV-peak is still unclear, there are several possibilities; One possibility is that the peak corresponds to blue luminescence in the $ZnGa_2O_4$ phase. Similarly, blue luminescence has been observed from $ZnGa_2O_4$ phosphors [32,33]. However, no $ZnGa_2O_4$ phase has been generated in our annealed sample, excluding this possibility. Second possibility is that the 2.8 eV-peak is attributed to the ZnO phase. The peak centered at 2.8 eV has been found, for the annealed ZnO nanoparticles [34]. In regard to the mechanism of the 2.8 eV luminescence, there are suggestions that it is associated with defects such as oxygen vacancies [35,36]. In particular, Heo et al. revealed that the emission peak (~2.8 eV) from ZnO nanorods grown using catalysis-driven molecular beam epitaxy is typically associated with trap-state emission being related to singly ionized oxygen vacancies in ZnO [35]. With the band gap of ZnO being 3.3 eV, the energy interval from the shallow donor level locating below the conductor band about 0.5 eV to the top of the valence band should be about 2.8 eV, which is consistent with the photon energy of the blue emission at 2.8 eV [36]. Liu et al. suggested that the blue emission at 2.8 eV is the result of the radiative overlap of the electron transition from the shallow donor level of oxygen vacancies and from the defect donor level associated with ionized oxygen vacancies to the valence band [36]. Accordingly, we suggest that thermal annealing induced the generation of oxygen vacancies in the ZnO shell layers, exhibiting the 2.8 eV-peak. Third possibility is that the 2.8 eV-peak is ascribed to the $Ga_2O_3$ core. Only a few papers have reported the 2.8 eV PL in nominally undoped $Ga_2O_3$. Shen et al. observed the 2.8 eV-peak from the undoped $Ga_2O_3$, which has been annealed [37]. It has been suggested that the blue emission of $Ga_2O_3$ is originated from the recombination of an electron on a donor formed by oxygen vacancies with a hole on an acceptor consisting of either gallium vacancies or gallium–oxygen vacancy pairs [4]. It is possible that the thermal annealing contributed to the generation of various vacancies, providing the 2.8 eV-peak. The identification of the physical origins of 2.8 eV luminescence found in the current study remains for future detailed systematic studies. Also, comparing Fig. 3c with Fig. 3b, it is found that the defect-related peaks (2.2 and 2.6 eV) have been intensified with respect to the UV peak. It is surmised that thermal annealing at 800 °C contributed to the generation of a variety of defects including vacancies.

The XRD spectrum of ZnO-coated $Ga_2O_3$ nanowires after thermal annealing is presented in Fig. 4. Some weak lines coincide with the (1 0 0), (0 0 2), (1 0 1), (1 0 2), (1 1 0), (1 0 3), and (1 1 2) peaks of the hexagonal structure of ZnO with lattice constants of $a = 3.249$ Å and $c = 5.205$ Å (JCPDS File No. 05-0664). No obvious reflection peaks from the impurities, such as unreacted Zn, Ga, or other zinc gallium oxides, were clearly detected, agreeing with the TEM investigations. [This part has been removed: On the other hand, comparing Fig. 3c with Fig. 3b, it is found that the defect-related

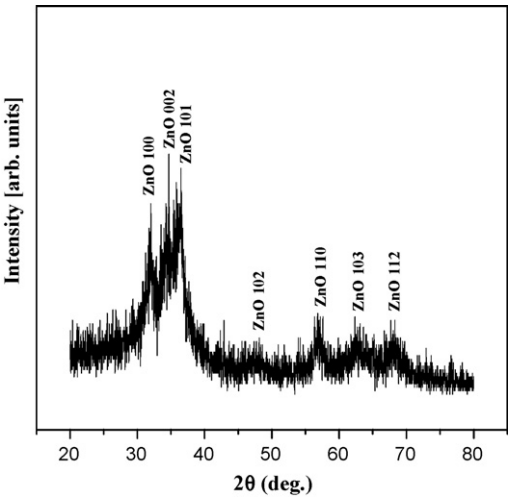


**Fig. 4.** XRD pattern of ZnO-coated $Ga_2O_3$ nanowires with subsequent thermal annealing at 800 °C.

peaks (2.2 and 2.6 eV) have been intensified with respect to the UV peak. It is surmised that thermal annealing at 800 °C contributed to the generation of a variety of defects including vacancies.].

## 4. Conclusions

We have prepared ZnO-coated $Ga_2O_3$ nanowires and subsequently investigated the effects of thermal annealing. XRD, SEM, TEM, and PL spectroscopy were employed to characterize the samples. SEM and TEM images indicate that the surface roughness of the nanowires was not significantly changed by the thermal annealing. SAED patterns and lattice-resolved TEM images reveal that the shell layer comprises a crystalline ZnO phase, regardless of whether the samples were annealed. The PL spectrum of ZnO-coated $Ga_2O_3$ core nanowires consists of four emission bands, at 3.2, 2.6, 2.2, and 1.6 eV. As a result of thermal annealing, defect-associated peaks (2.2 and 2.6 eV) have been intensified with respect to the UV peak, and a new 2.8 eV-peak has been generated. We suggested that the 2.8 eV-peak can be attributed to an emission from ZnO shell or $Ga_2O_3$ core.

## Acknowledgements

This work was supported by a Korea Research Foundation Grant funded by the Korean Government (MOEHRD) (KRF-2007-521-D00216). The main calculations were performed by the supercomputing resources of the Korea Institute of Science and Technology Information (KISTI).

## References

[1] M. Arnold, P. Avouris, Z.W. Pan, Z.L. Wang, J. Phys. Chem. B 107 (2003) 659.
[2] W.L. Hughes, Z.L. Wang, Appl. Phys. Lett. 82 (2003) 2886.
[3] X.D. Bai, E.G. Wang, P.X. Bai, Z.L. Wang, Appl. Phys. Lett. 82 (2003) 4806.
[4] L. Binet, D. Gourier, J. Phys. Chem. Solids 59 (1998) 1241.
[5] X. Xiang, C.-B. Cao, H.-S. Zhu, J. Cryst. Growth 279 (2005) 122.
[6] L.J. Lauhon, M.S. Gudiksen, D.L. Wang, C.M. Lieber, Nature 420 (2002) 57.
[7] Y. Yu, J. Xiang, C. Yang, W. Lu, C.M. Lieber, Nature 450 (2004) 61.
[8] H.-J. Choi, J.C. Johnson, R. He, S.-K. Lee, F. Kim, P. Pauzauskie, J. Golberger, R.J. Saykally, P. Yang, J. Phys. Chem. B 107 (2003) 8721.
[9] S. Han, C. Li, Z.Q. Liu, B. Lei, D.H. Zhang, W. Jin, X.L. Liu, T. Tang, C.W. Zhou, Nano Lett. 4 (2004) 1241.
[10] B. Min, J.S. Lee, J.W. Hwang, K.H. Keem, M.I. Kang, K. Cho, M.Y. Sung, S. Kim, M.-S. Lee, S.O. Park, J.T. Moon, J. Cryst. Growth 252 (2003) 565.
[11] K. Suenaga, C. Colliex, N. Demoncy, A. Loiseau, H. Pascard, F. Willaime, Science 278 (1997) 653.
[12] Y. Zhang, K. Suenaga, C. Colliex, S. Iijima, Science 281 (1998) 973.
[13] H.Y. Kim, S.Y. Bae, N.S. Kim, J. Park, Chem. Commun. 2003 (2003) 2634.
[14] H.W. Kim, S.H. Shim, J.W. Lee, Proc. SPIE 6423 (2007) 654.
[15] S.M. George, A.W. Ott, J.W. Klaus, J. Phys. Chem. 100 (1996) 13121.
[16] J.S. Lee, B. Min, K. Cho, S. Kim, J. Park, Y.T. Lee, N.S. Kim, M.S. Lee, S.O. Park, J.T. Moon, J. Cryst. Growth 254 (2003) 443.
[17] A.W. Ott, J.W. Klaus, J.M. Johnson, S.M. George, Thin Solid Films 292 (1997) 135.
[18] H.W. Kim, N.H. Kim, Appl. Surf. Sci. 230 (2004) 301.
[19] H.W. Kim, N.H. Kim, C. Lee, J. Mater. Sci. : Mater. El 16 (2005) 103.
[20] J. Lim, K. Shin, H. Kim, C. Lee, Thin Solid Films 475 (2005) 256.
[21] T. Harwig, F. Kellendouk, J. Solid State Chem. 24 (1978) 255.
[22] C.H. Liang, G.W. Meng, G.Z. Wang, Y.W. Wang, L.D. Zhang, S.Y. Zhang, Appl. Phys. Lett. 89 (2001) 3202.
[23] P. Guha, S. Chakrabarti, S. Chaudhurl, Physica E 23 (2004) 81.
[24] H.W. Kim, N.H. Kim, Appl. Phys. A 80 (2005) 537.
[25] J. Hu, Y. Bando, Z. Liu, Adv. Mater. 15 (2003) 1000.
[26] Y.P. Song, H.Z. Zhang, C. Lin, Y.W. Zhu, G.H. Li, F.H. Yang, D.P. Yu, Phys. Rev. B 69 (2004) 075304.
[27] P. Yang, H. Yan, S. Mao, R. Russo, J. Johnson, R. Saykally, N. Morris, J. Pham, R. He, H.-J. Choi, Adv. Funct. Mater. 12 (2002) 323.
[28] Q. Wan, Z.T. Song, W.L. Liu, C.L. Lin, T.H. Wang, Nanotechnology 15 (2004) 559.
[29] D.C. Reynolds, D.C. Look, B. Jogai, C.W. Litton, T.C. Collins, W. Harsch, G. Cantwell, Phys. Rev. B 57 (1998) 12151.
[30] S.W. Jung, W.I. Park, H.D. Cheong, G.-C. Yi, H.M. Jang, S. Hong, T. Joo, Appl. Phys. Lett. 80 (2002) 1924.
[31] J.S. Kang, H.S. Kang, S.S. Pang, E.S. Shim, S.Y. Lee, Thin Solid Films 443 (2003) 5.
[32] Y.E. Lee, D.P. Norton, C. Park, C.M. Rouleau, J. Appl. Phys. 89 (2001) 1653.
[33] I.-K. Jeong, H.L. Park, S.-I. Mho, Solid State Commun. 105 (1998) 179.
[34] G. Xiong, U. Pal, J.G. Serrano, K.B. Ucer, R.T. Williams, Phys. Stat. Sol. (c) 3 (2006) 3577.
[35] Y.W. Heo, M. Kaufman, K. Pruessner, D.P. Norton, F. Ren, M.F. Chisholm, P.H. Fleming, Solid State Electron. 47 (2003) 2267.
[36] D.H. Liu, L. Liao, J.C. Li, H.X. Guo, Q. Fu, Mater. Sci. Eng. B 121 (2005) 77.
[37] W.Y. Shen, M.L. Pang, J. Lin, J. Fang, J. Electrochem. Soc. 152 (2005) H25.